Volume 1 | Number 1 | Jan 2013 | Pages 1–100

Molecular Biosystems

www.rsc.org/molecularbiosystems

THE BIOLOGY OF PLAGUE

ROYAL SOCIETY OF CHEMISTRY
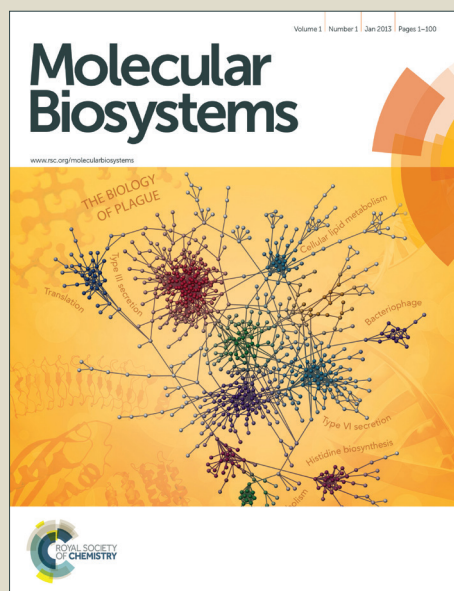
This is an *Accepted Manuscript*, which has been through the Royal Society of Chemistry peer review process and has been accepted for publication.

Accepted Manuscripts are published online shortly after acceptance, before technical editing, formatting and proof reading. Using this free service, authors can make their results available to the community, in citable form, before we publish the edited article. We will replace this *Accepted Manuscript* with the edited and formatted *Advance Article* as soon as it is available.

You can find more information about *Accepted Manuscripts* in the **Information for Authors**.

Please note that technical editing may introduce minor changes to the text and/or graphics, which may alter content. The journal's standard **Terms & Conditions** and the **Ethical guidelines** still apply. In no event shall the Royal Society of Chemistry be held responsible for any errors or omissions in this *Accepted Manuscript* or any consequences arising from the use of any information it contains.

- 1 -

Vitreous proteomic analysis of idiopathic epiretinal membrane

Jing Yu[*#], Le Feng[*], Yan Wu, Hao Wang, Jun Ba, Wei Zhu, Chunlei Xie

Department of Ophthalmology, Shanghai tenth People's Hospital, Tongji University School of

Medicine, Shanghai 200072 P. R. China

* Jing Yu, Le Feng contributed equally to this work.

Corresponding author: E-mail: dryujing@aliyun.com

Phone: 86-21-66301362

Fax: 86-21-66301362

The authors have declared no conflict of interest.

Running head: Vitreous proteomic analysis of iERM

KEYWORDS: *idiopathic epiretinal membrane, proteome, biomarker, estrogen receptor,*

ubiquitin-conjugating enzyme

- 2 -

Abstract

To understand the molecular mechanisms of idiopathic epiretinal membranes (iERM), the vitreous proteomes of patients with iERM were investigated. The vitreous proteome analysis in patients with iERM (n=8) and donor samples (n=8) was used by reversed phase high-performance liquid chromatography (RP-HPLC) coupled with electrospray Ionization tandem mass spectrometry (ESI-MS/MS) and analyzed by GeneGo Metacore^{TM}. This research followed the tenets of Declaration of Helsinki for the use of human subjects. In this current study, 226 significant changes in protein abundance (abundance ratio > 2, p < 0.01) were identified in vitreous from iERM patients compared to normal control vitreous, including 122 proteins that were present at lower levels and 104 proteins that were present at higher levels. In the iERM vitreous samples, complement components, inflammation-related proteins and matrix metalloproteinase were present at higher levels, while normal cytoskeleton proteins were present at lower levels. The top GeneGo pathway was "immune response", the top process network was "inflammation", and the top KEGG pathway was "coagulation cascades". The essential 2-node proteins of the network were estrogen receptor 1 (ESR1) and p300. Among the found at higher levels, ubiquitin- conjugating enzyme E2O (UBE2O) and complement C4A (C4A) were the most abundant proteins, and could be detected in each of the iERM vitreous samples. It can be concluded that iERM is a complicated pathological process involving inflammation, the immune response, and cytoskeleton remolding. UBE2O and C4A may be candidate biomarkers for iERM.

- 3 -

Epiretinal membrane formation characterizes a number of pathological changes occurring in the vitreoretinal junction with varying degrees of clinical significance[1, 2]. Idiopathic epiretinal membranes (iERM) can cause a reduction in vision and sometimes recur after surgical removal, but the pathogenic mechanisms that underlie this condition are still not well-known. iERM is a common vitreoretinal disease, and iERM patients are frequently used as the control group in studies of certain retinal diseases[3, 4]. iERM is essentially defined by an abnormal vitreoretinal appearance. Snead[5] found that laminocytes were the fundamental cell type involved in iERM. These cells were frequently found to be dispersed and present in reduced numbers in eyes containing a posterior vitreous detachment. The difference between proliferative vitreoretinopathy (PVR) and iERM is that the former includes the retinal pigment epithelial (RPE) cells, while the difference between proliferative diabetic retinopathy (PDR) and iERM is that the former involves neovascular stromal tissue. These cells have variously been reported as glial cells, glial fibroblasts, astrocytic cells, RPE cells, Müller cells and immune origin cells in previous studies[6-9]. These changes most likely represent an attempt to remodel the inner limiting membrane. The presence of type II collagen positivity in the laminocytes suggests that they may play an additional role of secreting collagen into the vitreous gel. These features clearly indicate that laminocytes have a central role in the pathology of iERM[10]. Previous studies have reported that specific cytokines are expressed in iERM, such as vascular endothelial growth factor[11, 12], interleukin-6[11], transforming growth factor-beta[12] and connective tissue growth factor[13]. However, there has been no systemic study on the changes in the vitreous proteins in iERMs.

Proteomic analysis is a powerful approach to determine the coordinated changes in protein levels in tissues and cells. Recent proteomic studies of human vitreous samples have revealed many proteins in patients with vitreoretinal disease[14-18]. Reversed phase high-performance liquid chromatography (RP-HPLC) coupled with electrospray Ionization tandem mass spectrometry (ESI-MS/MS) is a useful method for the analysis of the proteome of vitreous[19]. Pollreisz used quantitative liquid chromatography mass spectrometry (LCMS) and multiplex protein assays analysis of the aqueous (AF) and vitreous fluids (VF) from human eyes with iERM. A total of 323 proteins were identified in the AF and VF from eyes with iERM[20]. For the purpose of understanding the pathogenesis of iERM deeply, we employed this high-performance proteomic approach to analyze the vitreous humor of iERM patients using GeneGO MetaCore software.

MATERIALS AND METHODS

Vitreous Collection

Normal human eyes (control group) without any known ocular disease (n=8) that had been donated for corneal transplant in accordance with the Standardized Rules for Development and Applications of Organ Transplants were obtained from the Eye Bank of Shanghai in China. The mean post-mortem time was 3.1±0.8 hr (range: 2.3 to 4.0 hr). Eight iERM patients (iERM group) from Shanghai Tenth People's Hospital were enrolled in the study. The following enrollment and exclusion criteria were applied. Patients with ocular trauma, age-related macular degeneration, retinal vein occlusion, diabetes mellitus, a history of ocular surgery and other systemic diseases were excluded. The research was conducted in accordance with the tenets of the Declaration of Helsinki for the use of human subjects. Informed consent was obtained from all patients after a verbal and written explanation of the nature and possible consequences of the study had been provided. The ethics committee of the Tongji University School of Medicine approved the research protocol. In the iERM group, there are 4 males and 4 females and the mean age is 62.1± 6.3 years. While in the control group, there are 5 males and 3 females and the mean age is 57.2±7.3 years. There was no difference in the age and gender composition between the iERM patients and the control group (P>0.05).

The undiluted vitreous humor samples from iERM patients were collected using a method same as the previous Yu's research.[21] The harvested samples of vitreous humor were centrifuged for 15 min at 12,000 rpm to separate the cell contents, and they were stored at -80 °C until use.

Sample Preparation for MS Analysis

The samples preparation for MS analysis were same to that described in Wang's research.[21] The concentration of the iERM and control vitreous samples was adjusted to 5 μg/μl. Eight iERM vitreous samples and 8 control vitreous samples were pooled. The appropriate volumes of the mixed iERM and control vitreous samples were dissolved in a reducing solution (6 M urea, 2 M thiourea, Sigma, St Louis, MO). The supernatant was collected after centrifugation (12000 rpm, 30 min, 4). The protein concentration was determined using the Bradford protein assay. Forty

micrograms of protein from the samples of each fraction were reduced with 10 mM DTT (Sigma, St Louis, MO) at 37　for 2.5 h and alkylated with 50 mM iodoacetamide (Sigma, St Louis, MO) at room temperature for 40 min. After dilution in a solution of 25 mM NH_4HCO_3 (Sigma, St Louis, MO), the protein mixture was digested with sequencing-grade modified trypsin (Promega, Madison, WI) using a 1:50 enzyme: protein ratio at 37　for 20 h. The tryptic peptide mixture was lyophilized, dissolved with 0.1% formic acid, and then stored at -80　until use.

LC-ESI MS/MS Analysis

The Ettan MDLC controlled by UNICORN™ software (GE Healthcare, Piscataway, NJ), a system for automated micro- and nano-flow multi-dimensional chromatography was used for desalting and separation of tryptic peptides prior to online MS and MS/MS analyses. In this system, samples were desalted on RP trap columns (Zorbax 300 SB C18, Agilent Technologies, Palo Alto, CA), and separated on an RP column (150 μm × 150 mm, Column Technology Inc., Fremont, CA). Mobile phase A (0.1% formic acid in HPLC-grade water) and the mobile phase B (0.1% formic acid in acetonitrile) were selected. The tryptic peptide mixtures were eluted using a gradient of 2-98% B over 180 min. The RP-HPLC was coupled on-line with an ESI-linear ion-Trap mass spectrometer (LTQ, Thermo Fisher Scientific, Waltham, MA) for MS and MS/MS analysis. The nanoelectrospray source was operated at 2.1 kV, with no sheath gas flow and with the ion transfer tube at 200 ℃. Data-dependent MS/MS spectra were obtained simultaneously. Each scan cycle consisted of one full MS scan in profile mode followed by ten MS/MS scans on the 10 most intense ions from the MS spectrum with the following Dynamic Exclusion settings: repeat count 2, repeat duration 30 s, exclusion duration 90s.[22] Each sample was analyzed in triplicate.

Data Analysis and Label-Free Quantitation

A Finnigan LTQ linear ion trap MS (Thermo Electron, San Jose, CA) equipped with an electrospray interface was connected to the LC setup for eluted peptide detection. Each sample was analyzed in triplicate. All MS/MS data were investigated using the Mascot search engine (version 2.0, Matrix Science, Boston, MA) against the human International Protein Index (IPI) protein sequence database (IPI version 3.60), and the search results obtained for the peptide MS/MS assignment were filtered based on the criterion defined as a Mascot peptide score more than 20. Peptide

- 6 -

detection, background subtraction and quantitation were performed on the full scan precursor mass

spectra in fully automatic mode using DeCyder MS differential analysis software (version 2.0, GE

Healthcare).

Bioinformatics Analysis

Gene Ontology (GO) enrichment/depletion analysis

To prepare an overview of our proteomic analysis of iERM, we categorized the specific proteins of

iERM based on their GO assignments. GeneGo Metacore^{TM} (Version: 6.5) was used for the

enrichment workflow analysis. For the enrichment/depletion analysis, a test dataset composed of

the identified proteins and a reference set of annotated proteins from the complete human proteome

were needed. According to the instructions on the GO fact webpage, the custom GO annotation for

the reference set (of whole IPI human dataset) was created by extracting the GO annotations with

GOA (http://www.ebi.ac.uk/GOA) according to their IPI IDs. The analysis was performed using R

scripts with the hypergeometric test and FDR correction; the GO terms with $P < 0.05$ were selected

as enriched/depleted or significantly enriched/depleted. The cellular component (CC), molecular

function (MF) and biological process (BP) of the selected proteins were annotated using the GO

database.

Pathway analysis

ArrayTrack software was used for pathway analysis. ArrayTrack offers a simple query interface to

retrieve information about human protein expression profiles and provides direct connections to

related biological pathways available from the Kyoto Encyclopedia of Genes and Genomes

(KEGG). Based on the ArrayTrack manual, the IPI names of the differentially expressed proteins

were converted to SWISS-PROT names using the ID convert tool prior to pathway analysis and then

entered into the Pathway Search panel. For the statistical analysis, a p value for pathway enrichment

was obtained using Fisher's exact test, and a p value <0.05 was considered statistically significant.

Western Blot Analysis

Since estrogen receptor 1 (ESR1) and tubulin were the key nodes of the direct interaction network,

while ubiquitin-conjugating enzyme 2O (UBE2O) and complement C4A (C4A) were the proteins

significant changes in protein abundance to 100 folds and 50 folds, respectively, therefore the four

proteins were selected to verify the unique proteins in proteome by performing the Western Blotting

analysis. The primary antibodies were showed as the following: ESR1 (R&D Systems, USA,

1:300), tubulin (Abcam, Cambridge, UK, 1:500), C4A (Novus Biologicals, USA, 1:300), and

UBE2O (Novus Biologicals, USA, 1:300).

The same amount of the protein (10 μg) from each vitreous sample (n =16) was applied to each lane

of a 10% acrylamide gel and then electrophoretically transferred to a polyvinylidene fluoride

transfer membrane (Hybond-C; Amersham Biosciences Inc., Arlington Heights, IL) at 80 mV for 1

h. The membranes were blocked with 5% BSA (w/v) for 1 h at room temperature and incubated

overnight at 4 ℃ with the primary antibodies. The blots were washed with PBS-T (0.1% Tween-20

in PBS) three times before incubating with IRDye 680 donkey anti-mouse, IRDye 800 donkey

anti-rabbit or IRDye 800 donkey anti-goat (diluted to 1:1000; LI-COR Biosciences) for 1 h at room

temperature. The hybridized membrane was washed in PBS-T buffer and scanned using the

Odyssey infrared imaging system (LI-COR, Lincoln, NE) at a wavelength of 700 to 800 nm. The

Western blot density data between the groups were compared with the Mann-Whitney U test.

Statistical Analysis

The Student t-test, chi-squared test, Fisher's exact test, and Mann-Whitney U test were performed in

the current study (SPSS 14.0, Chicago, IL, USA). A p value <0.05 was considered statistically

significant.

RESULTS

Average vitreous protein concentration

The average vitreous protein concentration in the iERM samples (4.11±1.19 mg/ml) was

significantly higher than in the control samples (2.98 ± 1.23 mg/ml) (t =2.145, p= 0.036) (Figure

1A).

The Integrated Proteome

The integrated 412 unique proteins were unambiguously identified by LC-ESI MS/MS in control

and iERM vitreous samples. Compared with the control proteome, 179 proteins were present at

higher levels and 233 proteins were present at lower levels in the iERM proteome. In the current

- 8 -

study, 226 significant changes in protein abundance (abundance ratio > 2, p < 0.01) were identified

in vitreous from iERM patients compared to normal control vitreous, including 122 proteins that

were present at lower levels and 104 proteins that were present at higher levels. (Figure 1B). Among

the proteins at lower leverls with a 2-fold change, the proteins with a molecular weight (MW) of

less than 60 kDa composed the majority (62.9%) compared with the proteins (51.9%) (Fisher's

exact, *p*=0.138). (Figure 1C) Furthermore, the percent of proteins with a isoelectric point (PI) less

than 7 (53.3%) in the proteins at lower leverls was greater than that in the proteins at higher

leverls (46.2%) (Fisher's exact, *p*=0.500). (Figure 1D) The proteins that presented at least a 2-fold

change are shown in Supplemental Figure 1. Several cytoskeleton proteins, such as tubulin,

albumin, and crystallin, were presented at significantly lower levels (over 10-fold). Proteins,

which induced the degradation of the extracellular matrix, such as matrix metalloproteinase

(MMP)-28 (3.99-fold), were presented at significantly higher levels. The proteins involved in

inflammation and signal transduction, such as alpha-1-antichymotrypsin, complement C4A and

protein tyrosine kinase, were presented at significantly higher levels (over 10-fold). These results

suggested that the normal cytoskeleton was degraded due to the activation of inflammation. The

proteins present 10-fold higher levels or lower levels are shown in Table 1. The database

information of the proteins present 2-fold higher or lower levels in the iERM vitreous proteome

were presented in Supplemental Table 1 and 2.

GO Analysis

Based on the terms represented in the GO database, the differentially expressed proteins were

divided into 3 categories: cellular component (CC), molecular function (MF) and biological

process (BP). The proteins in the iERM vitreous proteome presented 2-fold levels changed were

analyzed. The CC, MF and BP of level 2 were compared between the iERM and donor proteome.

In this case, the significantly decreased proteins were defined as those for which the percentage of

proteins at lower levels minus the percentage of proteins at higher levels was no less than 5%. The

significantly increased proteins were defined as those for which the percentage of proteins at

higher levels minus the percentage of proteins at lower levels was no less than 5%. The proteins

with the MFs related to catalytic activity, enzyme regulator activity, binding and structural

molecule activity were significantly decreased. (Figure 2A) The proteins with the BPs involving

- 9 -

cellular processes, multicellular organismal processes, metabolic process, cellular organization or biogenesis, response to stimuli, biological regulation, establishment of localization, signaling and localization were significantly decreased. (Figure 2B) The proteins with CC of extracellular region part, extracellular region, organelle part, organelle, cell part and cell were significantly decreased. (Figure 2C). However, no proteins with MFs or BP or CC were significantly increased over 5%. The results suggested that in the iERM process, the proteins with structural and metabolic functions were decreased. Furthermore, the proteins changed not only in cell, but also in extracellular region.

GeneGo Analysis

The GeneGo pathway maps for the iERM samples were ranked in terms of the enrichment of the differentially expressed proteins (*p*-value), and the top 5 networks were immune response (alternative complement pathway), immune response (lectin-induced complement pathway), blood coagulation, immune response (classical complement pathway) and transcription (Role of Akt in hypoxia induced by H1F1 activation). The GeneGo process networks for the iERM samples were ranked in terms of the enrichment of the differentially expressed proteins (*p*-value), and the top 5 networks were inflammation (kallikrein-kinin system, KKS), inflammation (complement system), cytoskeleton (regulation of cytoskeleton rearrangement), inflammation (IL-6 signaling) and blood coagulation. In iERM vitreous, the top 3 significant pathways were complement and coagulation cascades (hsa04610, p=1.22E-05), glycolysis/gluconeogenesis (hsa00010, p=2.91E-05), and phagosome (hsa04145, p=0.0016). There were 10 proteins detected in the complement and coagulation cascades, including coagulation cascade (SERPNC1, SERPNA1, A2M, F2, FG), kallikrein-kinin system (KNG, PLG) and complement cascade (C3, C4, SERPNG1). (Figure 2) Interaction networks exist among the proteins of the vitreous proteome. The top 5 key node proteins in this network were ESR1 (nuclear), p300, CBP, thrombin and tubulin (in microtubules). The direct interaction network is shown in Figure 3.

Verification of the Proteins Identified in iERM Samples by Western Blotting Analysis

The four proteins, ESR1, tubulin, UBE2O, and C4A, were detected in all iERM (n=8) and control

vitreous samples (n=8). The changes in protein abundance noted in the western blot analysis were highly consistent with the results of the proteomic screening. As shown in Figure 4, tubulin (the density control vs iERM: 57.86±16.72 vs 16.3±11.13) and ESR1 (control vs iERM: 39.12±17.35 iERM: 6.69±1.31) were significantly lower, while UBE2O (control vs iERM: 9.03±0.32 vs 10.76±0.79) and C4A (control vs iERM: 7.75±0.63 vs 11.97±1.45) were significantly higher in the iERM group compared with the controls when the data were analyzed with the Mann-Whitney U test ($p < 0.05$).

DISCUSSION

Since the vitreous is the place where the retinal diseases happen, the change of the vitreous proteins could affect the pathological mechanism and development of the diseases. Therefore, it is essential to study the proteome of the vitreous. In the current proteomic study of iERM pateints, Pollreisz found that the proteins expressed difference in the aqueous (AF) and vitreous fluids (VF). The levels of some cytokines and growth factors, such as Flt3, PDGF, ICAM1 and IL-7 were expressed higher in VF than that in AF [20]. In the present study, we performed a systematic proteomic comparison of vitreous from iERM patients and normal controls. Integration of the datasets from the control and iERM proteomes will result in a comprehensive understanding of the protein functions of a given biofluid. There were 412 distinct proteins identified by LC-ESI MS/MS in the integrated donor and iERM vitreous samples. In the iERM vitreous proteome, more proteins were at lower levels (233 proteins), although some proteins were at higher levels (179 proteins) compared with the normal vitreous proteome. The results suggested that iERM is characterized by a complicated process that involves changes in the levels of a large number of proteins.

Clinically, iERM is frequently used as the control group when studying certain retinal diseases[3, 4]. However, iERM is a certain proliferative disease in essence. In the current study, the average vitreous protein concentrations in iERM samples were significantly higher than those in control samples. Furthermore, a great amount of the proteins were changed in protein abundance in the iERM vitreous proteome. Zhang also found that there was no statistically significant difference in the cell proliferative index between PVR (70.1 ± 4.2%), PDR (82.1 ± 7.0%) and iERM (72.9 ± 22.8%), which indicated that iERM was a certain of proliferative diseases similar with PVR or

- 11 -

PDR[23] . In the epiretinal membranes of PVR, PDR, and iERM patients, cell proliferation and apoptosis appeared to be key mechanisms regulating certain cell populations. In previous studies, several cytokines, such as vascular endothelial growth factor[11, 12], transforming growth factor-beta [11], interleukin-6 [12], chemokine CCL2 [24] and tumor necrosis factor-alpha[24] , have been detected in the iERM. However, these cytokines were not found in the iERM vitreous proteome.

Epiretinal membrane formation requires cell migration and proliferation, extracellular matrix formation and tissue contraction. The plasminogen activator-mediated proteolytic cascade is an important mechanism for pericellular degradation of the extracellular matrix. Immonen found that urokinase and tissue-type plasminogen activator were present in the iERM.[25] In our study, plasminogen and matrix metalloproteinase-28 were detected in the iERM vitreous proteome. Meanwhile, most cytoskeleton proteins were presented at significantly lower levels. This suggested that normal cytoskeleton vitreous proteins changed significantly in iERM process. Previous reports have demonstrated that the extracellular matrix components fibronectin (FN), laminin, and vitronectin were the major components of the epiretinal and subretinal membranes of PVR, which were detected in vitreous[26, 27]. However, in our study, only FN was detected in iERM vitreous, which was increased over 2-fold. It is possible that continuous tissue remodeling with simultaneous extracellular matrix production and breakdown regulate the growth of epiretinal membranes.

Another crucial finding in our study was that the immune response, including the alternative complement pathway, the lectin-induced complement pathway and the classical complement pathway, was important in the iERM process. It was supported another current iERM proteomic study outcomes which the classical and alternative pathway of complement activation was the top biological process[20]. There were 5 complement proteins, including C4A, C3, complement factor B, detected in iERM vitreous in our study. Among them, C4A was presented at 50-fold higher levels compared with the normal vitreous proteome. Meanwhile, inflammation was the most affected process network, which could be induced by the complement system, KKS and interleukin-6. Therefore, our results suggested that the inflammation that occurs in iERM could involve the complement and coagulation cascades pathway. Interestingly, this pathway was one of the key pathways involved in PVR [28] and PDR [29] in our other studies. Therefore, we suppose that the

complement and coagulation cascades pathway may be common among the retinal proliferative diseases.

In our current study, the protein abundance of UBE2O was presented at 100-fold higher levels in the iERM proteome comparing the normal control group. Meanwhile, the western blot analysis also detected that UBE2O expression was significantly higher in the iERM vitreous samples than in the control group. Ubiquitination is one of the most important post-translational modifications in all eukaryote organisms. The addition of ubiquitin moieties to proteins is carried out by the sequential action of three enzymes, ubiquitin-activating enzyme (E1), ubiquitin-conjugating enzyme (E2), and ubiquitin ligase (E3). E2 conjugating enzymes are the central enzymes in the ubiquitination pathway and are responsible for the transfer of ubiquitin and ubiquitin-like proteins onto target substrates[30]. Post-translational modification of proteins by ubiquitin (Ub) regulates a host of cellular processes, including protein quality control, DNA repair, endocytosis, and cellular signaling[31]. Protein misfolding and subsequent aggregation are hallmarks of several human diseases. Cells have a variety of mechanisms for coping with misfolded protein stress, including ubiquitin-mediated protein degradation. Our results indicated that ubiquitination was one of the key mechanisms in the pathogenesis of iERM, which can result in the degradation of normal proteins and new proteins production. It was reported that the ubiquitin-conjugating enzyme E2N was significantly over-expressed in gastric adenocarcinoma and could be a possible diagnostic biomarker of this disease[32]. However, whether UBE2O could be a protein biomarker of iERM should be validated in larger samples.

In the current study, ESR1 was the key node protein in the direct interaction network of the iERM proteome. The protein abundance of ESR1 was presented at 4.65-fold lower levels decreased in iERM vitreous. Estrogens are critical for sexual differentiation; in addition, it is well-known that 17β-estradiol modulates memory, learning, and mood in the adult brain and acts as a neuroprotector[33]. It exerts its actions through two classical receptors: estrogen receptor alpha (ERα, ESR1) and estrogen receptor beta (ERβ, ESR2). Estrogen and its receptors have been implicated in the development of many types of malignant tumors during recent years[34]. Functionally, the activation of ESR1 is associated with the proliferation and growth of tumor cells[35, 36], whereas the activation of ESR2 promotes apoptosis, suppresses malignant transformation and inhibits the growth of tumor cells[37]. The research showed that the estrogen network is assembled around the

- 13 -

core with other modules essential for all phases of the cell cycle[38]. Marin-Castano et al[39] have previously reported that both ESR1 and ESR2 are expressed in vitro and in vivo in human RPE cells, and the presence of both subtypes would predict a more complex regulation of estrogen-mediated gene expression. The distribution of both receptors changes from one brain area to another, and 17β-estradiol is able to modulate their expression. It was reported that estrogen is implicated in the development or progression of a number of human cancers (breast, ovarian, colorectal, prostate, and endometrial), endometriosis, fibroids, and cardiovascular disease[40]. Therefore, ESR1 may be a potential target in the treatment of iERM.

However, there are several limitations in our study. The number of iERM samples was relatively small. No experiment was performed to determine whether the unique proteins in the vitreous are expressed in the serum of iERM patients. Further research should include larger samples to elucidate the feasibility of these special proteins as serum biomarkers.

Conclusions

It can be concluded that iERM is a complicated pathological process involving large number of proteins that participate in inflammation, immune reactions, and cytoskeleton remolding. The KEGG pathway of "complement and coagulation cascades" leading to stimulation of an immune response and inflammation may play a crucial role in the pathological process of iERM. UBE2O and C4A may be candidate biomarkers for iERM. Further investigations of these proteins will provide additional targets for the treatment and prevention of iERM.

Author Contributions

Conceived and designed the experiments: JY.

Collected samples: LF HW JB CLX

Performed the experiments: LF YW JB WZ.

Analyzed the data: JY LF HW YW.

Contributed reagents /materials /analysis tools: JY LF HW JB.

Wrote the paper: JY LF.

- 14 -

Acknowledgement

REFERENCES

1.   R. Y. Foos, *Albrecht Von Graefes Arch Klin Exp Ophthalmol*, 1974, **189**, 231-250.

2.   A. M. Roth and R. Y. Foos, *Trans Am Acad Ophthalmol Otolaryngol*, 1971, **75**, 1047-1058.

3.   Y. Ma, Y. Tao, Q. Lu and Y. R. Jiang, *Am J Ophthalmol*, 2011, **152**, 678-685 e672.

4.   Y. Suzuki, M. Nakazawa, K. Suzuki, H. Yamazaki and Y. Miyagawa, *Jpn J Ophthalmol*, 2011, **55**, 256-263.

5.   D. R. Snead, S. James and M. P. Snead, *Eye (Lond)*, 2008, **22**, 1310-1317.

6.   W. E. Smiddy, A. M. Maguire, W. R. Green, R. G. Michels, Z. de la Cruz, C. Enger, M. Jaeger and T. A. Rice, *Ophthalmology*, 1989, **96**, 811-820; discussion 821.

7.   P. S. Hiscott, I. Grierson, C. J. Trombetta, A. H. Rahi, J. Marshall and D. McLeod, *Br J Ophthalmol*, 1984, **68**, 698-707.

8.   A. Kampik, W. R. Green, R. G. Michels and P. K. Nase, *Am J Ophthalmol*, 1980, **90**, 797-809.

9.   S. Y. Oberstein, J. Byun, D. Herrera, E. A. Chapin, S. K. Fisher and G. P. Lewis, *Mol Vis*, 2011, **17**, 1794-1805.

10.   G. A. Williams, *Br J Ophthalmol*, 2006, **90**, 1216-1217.

11.   E. Mandelcorn, Y. Khan, L. Javorska, J. Cohen, D. Howarth and M. Mandelcorn, *Can J Ophthalmol*, 2003, **38**, 457-463.

12.   T. Yamamoto, N. Akabane and S. Takeuchi, *Am J Ophthalmol*, 2001, **132**, 369-377.

13.   E. J. Kuiper, M. D. de Smet, J. C. van Meurs, H. S. Tan, M. W. Tanck, N. Oliver, F. A. van Nieuwenhoven, R. Goldschmeding and R. O. Schlingemann, *Arch Ophthalmol*, 2006, **124**, 1457-1462.

14.   R. E. Neal, F. A. Bettelheim, C. Lin, K. C. Winn, D. L. Garland and J. S. Zigler, Jr., *Exp Eye Res*, 2005, **80**, 337-347.

15.   M. Ouchi, K. West, J. W. Crabb, S. Kinoshita and M. Kamei, *Exp Eye Res*, 2005, **81**, 176-182.

16.   C. W. Wu, J. L. Sauter, P. K. Johnson, C. D. Chen and T. W. Olsen, *Am J Ophthalmol*, 2004, **137**, 655-661.

17.   K. Yamane, A. Minamoto, H. Yamashita, H. Takamura, Y. Miyamoto-Myoken, K. Yoshizato, T. Nabetani, A. Tsugita and H. K. Mishima, *Mol Cell Proteomics*, 2003, **2**, 1177-1187.

18.   F. H. Grus, S. C. Joachim and N. Pfeiffer, *Proteomics Clin Appl*, 2007, **1**, 876-888.

19.   M. Munoz, F. J. Corrales, J. N. Caamano, C. Diez, B. Trigal, M. I. Mora, D. Martin, S. Carrocera and E. Gomez, *J Proteome Res*, 2012, **11**, 751-766.

20.   A. Pollreisz, M. Funk, F. P. Breitwieser, K. Parapatics, S. Sacu, M. Georgopoulos, R. Dunavoelgyi, G. J. Zlabinger, J. Colinge, K. L. Bennett and U. Schmidt-Erfurth, *Exp Eye Res*, 2013, **108**, 48-58.

21.   J. Yu, F. Liu, S. J. Cui, Y. Liu, Z. Y. Song, H. Cao, F. E. Chen, W. J. Wang, T. Sun and F. Wang,

- 15 -

Proteomics, 2008, **8**, 3667-3678.

22. H. Wang, L. Feng, J. Hu, C. Xie and F. Wang, *Exp Eye Res*, 2012, **108C**, 110-119.

23. X. Zhang, G. Barile, S. Chang, A. Hays, S. Pachydaki, W. Schiff and J. Sparrow, *Curr Eye Res*, 2005, **30**, 395-403.

24. D. Armstrong, A. J. Augustin, R. Spengler, A. Al-Jada, T. Nickola, F. Grus and F. Koch, *Ophthalmologica*, 1998, **212**, 410-414.

25. I. Immonen, A. Vaheri, P. Tommila and V. Siren, *Graefes Arch Clin Exp Ophthalmol*, 1996, **234**, 664-669.

26. E. Ioachim, M. Stefaniotou, S. Gorezis, E. Tsanou, K. Psilas and N. J. Agnantis, *Eur J Ophthalmol*, 2005, **15**, 384-391.

27. I. Immonen, K. Tervo, I. Virtanen, L. Laatikainen and T. Tervo, *Acta Ophthalmol (Copenh)*, 1991, **69**, 466-471.

28. J. Yu, R. Peng, H. Chen, C. Cui and J. Ba, *Invest Ophthalmol Vis Sci*, 2012, **53**, 8146-8153.

29. H. Wang, L. Feng, J. W. Hu, C. L. Xie and F. Wang, *Proteome Sci*, 2012, **10**, 15.

30. C. Chapard, D. Hohl and M. Huber, *Exp Dermatol*, 2012, **21**, 321-326.

31. A. Arrigoni, B. Grillo, A. Vitriolo, L. De Gioia and E. Papaleo, *J Struct Biol*, 2012, **178**, 245-259.

32. N. Kocevar, F. Odreman, A. Vindigni, S. F. Grazio and R. Komel, *World J Gastroenterol*, 2012, **18**, 1216-1228.

33. A. Navarro, E. Del Valle, C. Ordonez, E. Martinez, C. Perez, A. Alonso, C. Gonzalez and J. Tolivia, *Age (Dordr)*, 2012.

34. G. G. Chen, Q. Zeng and G. M. Tse, *Med Res Rev*, 2008, **28**, 954-974.

35. Y. Zhang, Q. Liao, C. Chen, L. Yu and J. Zhao, *Int J Gynecol Cancer*, 2006, **16**, 1656-1660.

36. Z. Lin, S. Reierstad, C. C. Huang and S. E. Bulun, *Cancer Res*, 2007, **67**, 5017-5024.

37. O. Treeck, G. Pfeiler, F. Horn, B. Federhofer, H. Houlihan, A. Vollmer and O. Ortmann, *Mol Cell Endocrinol*, 2007, **264**, 50-60.

38. Y. Nikolsky, S. Ekins, T. Nikolskaya and A. Bugrim, *Toxicol Lett*, 2005, **158**, 20-29.

39. M. E. Marin-Castano, S. J. Elliot, M. Potier, M. Karl, L. J. Striker, G. E. Striker, K. G. Csaky and S. W. Cousins, *Invest Ophthalmol Vis Sci*, 2003, **44**, 50-59.

40. K. A. Burns and K. S. Korach, *Arch Toxicol*, 2012, **86**, 1491-1504.

- 16 -

Tables

Table 1 The proteins present at 10-fold higher levels (Ratio <0.1) or10-fold lower levels (Ratio>10) in iERM proteome relative to normal controls. (Ratio: control/iEMM)

	N	Symbols	In detail	Ratio
Proteins at higher levels	1	UBE2O	ubiquitin-conjugating enzyme E2O	0.01
	2	C4A	complement C4A	0.02
	3	SERPINA3	alpha-1-antichymotrypsin	0.02
	4	CPS1	CPS1 protein	0.03
	5	PTK2	protein tyrosine kinase 2	0.04
	6	EP300	histone acetyltransferase p300	0.04
	7	MAP1A	microtubule-associated protein 1A	0.04
	8	DUSP5	dual specificity protein phosphatase 5	0.05
	9	ZNF192	zinc finger protein 192	0.06
	10	TKT	transketolase	0.07
	11	C1orf228	uncharacterized protein C1orf228	0.08
	12	ORM2	orosomucoid 1 precursor	0.10
Proteins at lower levels	1	TTR	transthyretin	10.19
	2	DYNC1LI2	cytoplasmic dynein 1 light intermediate chain 2	11.19
	3	PTGDS	prostaglandin-H2 D-isomerase	11.83
	4	CKB	creatine kinase B-type	12.92
	5	TUBB2C	tubulin beta-2C chain	13.16
	6	PPIA	peptidyl-prolyl cis-trans isomerase A	13.32
	7	GBP3	guanylate binding protein 3	14.69
	8	TRIM41	putative uncharacterized protein TRIM41	15.23
	9	HSP90AA1	heat shock 90kDa protein 1	15.50
	10	Calsequestrin	calsequestrin	16.19
	11	PRICKLE4	cDNA FLJ32622 fis	16.79
	12	ALB	albumin	17.53
	13	CRYBA1	beta-crystallin A3	17.98
	14	SERPINC1	antithrombin-III	18.79
	15	FAM75A7	protein FAM75A7	20.63
	16	CRYBB1	beta-crystallin B1	28.36
	17	NR2C2	nuclear receptor subfamily 2 group C	41.34
	18	AGAP1	117 kDa protein	57.77
	19	HUNK	hormonally up-regulated neu tumor-associated kinase	91.42
	20	HOOK3	protein Hook homolog 3	117.07
	21	PRG4	proteoglycan 4	257.79

Legends

Figure 1 Integrated analysis of proteome data from control and iERM vitreous. (A) Average

protein concentrations in control and iERM samples. The average vitreous protein concentration

in the iERM samples was significantly higher than in the control samples (p<0.05). (B) The

diagram shows the proteins identified in the control and iERM samples. The numbers in the large

circle show the proteins that were present at higher or lower levels in the iERM samples relative to

controls. The numbers in the small oval show the proteins that were present at higher or lower

levels relative to controls based on a more than 2-fold difference in the iERM samples. (C) The

MW of the proteins present at 2-fold higher levels or 2-fold lower levels in the iERM samples. (D)

The PI of the proteins present at 2-fold higher levels or 2-fold lower levels in the iERM samples.

Figure 2 The proteins abundance significant changed difference more than 5% based on MF, BP

or CC. The number over the bar is the value of the percentage.

Figure 3 The complement and coagulation cascades pathway in the iERM vitreous proteome. In

the pathway, coagulation cascade, KKS and complement cascade were included. The proteins in

red are proteins that were detected in the iERM proteome. (KNG, kininogen; SERPIN, serpin

peptidase inhibitor; BF, complement factor B; HF, complement factor H; IF, complement factor I;

A2 M, alpha-2-macroglobulin; F2, thrombin; FG, fibrinogen alpha chain).

Figure 4 The direct interaction network in iERM vitreous proteome.

ESR1 (nuclear), 30 edges; p300, 20 edges; CBP, 11 edges;

Thrombin, 8 edges; Tubulin (in microtubules), 8 edges.

Figure 5 Proteins were identified by Western blotting. A (tubulin), B (ESR1), C (C4a), D

(UBE2O). The results are expressed as the means ± SD. *, p < 0.05.

Supplemental data:

Figure 1 The GO categories and gene sources of the proteins present at 2-fold higher levels or

lower levels.

Table 1 The database information of the proteins present 2-fold higher levels in the iERM vitreous

proteome.

Table 2 The database information of the proteins present 2-fold lower levels in the iERM vitreous
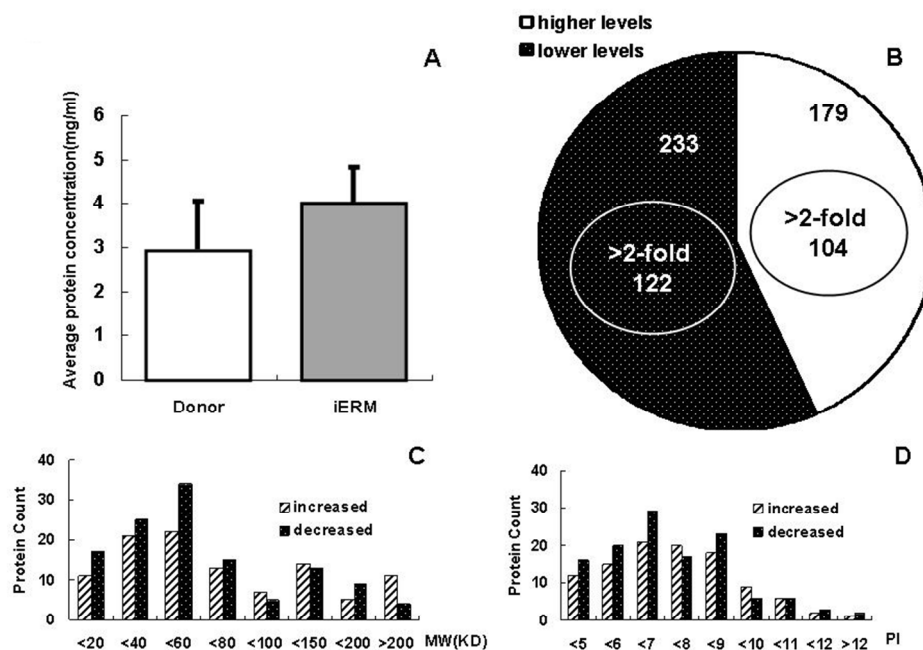
proteome.

Figure 1 Integrated analysis of proteome data from control and iERM vitreous. (A) Average protein concentrations in control and iERM samples. The average vitreous protein concentration in the iERM samples was significantly higher than in the control samples (p<0.05). (B) The diagram shows the proteins identified in the control and iERM samples. The numbers in the large circle show the proteins that were present at higher or lower levels in the iERM samples relative to controls. The numbers in the small oval show the proteins that were present at higher or lower levels relative to controls based on a more than 2-fold difference in the iERM samples. (C) The MW of the proteins present at 2-fold higher levels or 2-fold lower levels in the iERM samples. (D) The PI of the proteins present at 2-fold higher levels or 2-fold lower levels in the iERM samples.
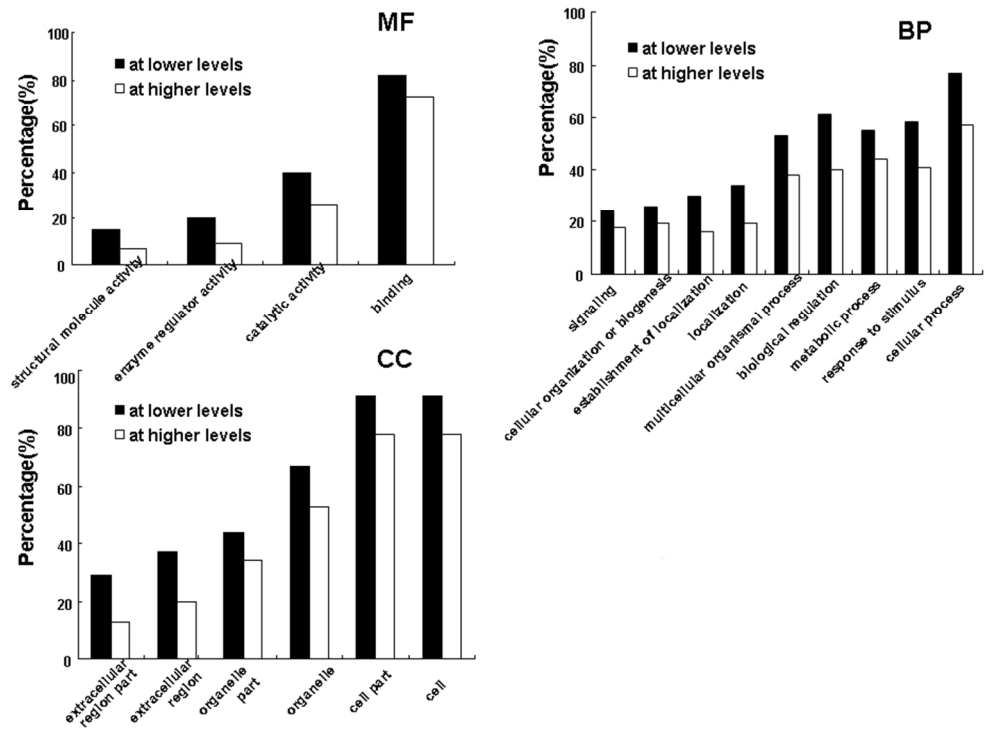255x183mm (96 x 96 DPI)

Figure 2 The proteins abundance significant changed difference more than 5% based on MF, BP or CC. The number over the bar is the value of the percentage.
249x181mm (96 x 96 DPI)

Figure 3 The complement and coagulation cascades pathway in the iERM vitreous proteome. In the pathway, coagulation cascade, KKS and complement cascade were included. The proteins in red are proteins that were detected in the iERM proteome. (KNG, kininogen; SERPIN, serpin peptidase inhibitor; BF, complement factor B; HF, complement factor H; IF, complement factor I; A2 M, alpha-2-macroglobulin; F2, thrombin; FG, fibrinogen alpha chain).
254x190mm (96 x 96 DPI)

Figure 4 The direct interaction network in iERM vitreous proteome.
ESR1 (nuclear), 30 edges;   p300, 20 edges;   CBP, 11 edges;
Thrombin, 8 edges;   Tubulin (in microtubules), 8 edges.
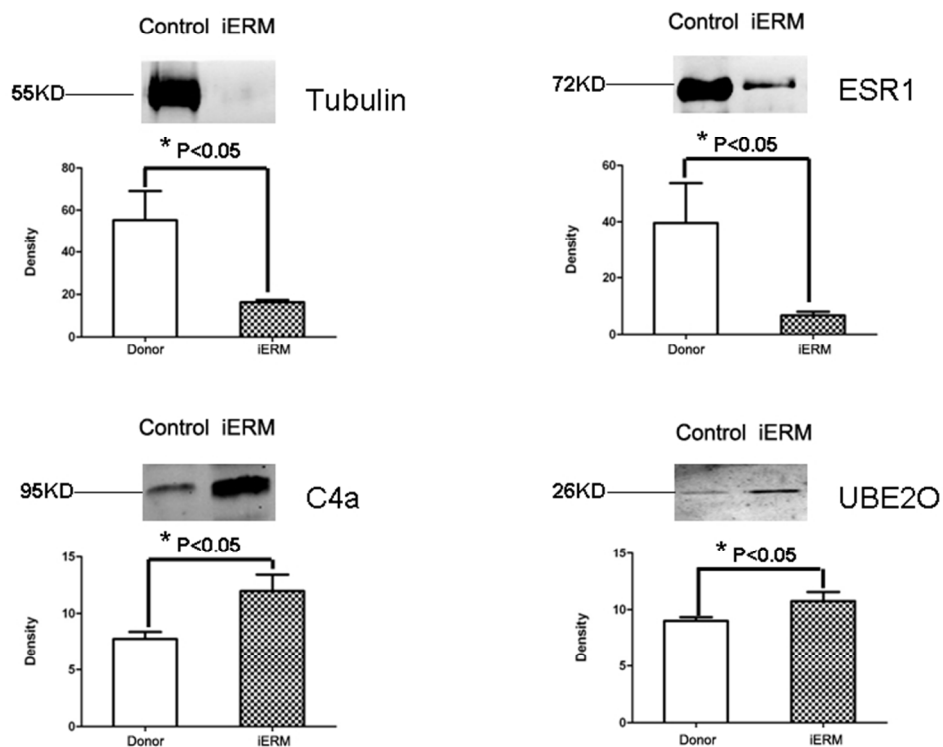123x97mm (96 x 96 DPI)

Figure 5 Proteins were identified by Western blotting. A (tubulin), B (ESR1), C (C4a), D (UBE2O). The results are expressed as the means ± SD. *, p < 0.05
209x173mm (96 x 96 DPI)